From Bq cm^{-3} to Bq cm^{-2} (and conversely)-part 1: a useful conversion for autoradiography

Sophie Billon, Paul Sardini, Sylvain Leblond, Pascal Fichet

From Bq cm^{-3} to Bq cm^{-2} (and conversely) - Part 1: a useful conversion for autoradiography

Sophie Billon[1], Paul Sardini[2], Sylvain Leblond[3], Pascal Fichet[3]

[1] *ERM company, rue Michel Brunet, Bat. 35, 86000 Poitiers, France*

[2] *Université de Poitiers, UMR 7285 CNRS, IC2MP, rue Michel Brunet, Bat. 35, 86073 Poitiers cedex 9, France*

[3] *Den-SEARS, CEA, Université Paris-Saclay, F-91191, Gif Sur Yvette, France*

sophie.billon@erm-poitiers.fr

Abstract

Autoradiography technique generally provides an image in cps cm^{-2}, the conversion in Bq g^{-1} remaining a challenge. The Geant4 tool has been used to establish a conversion procedure based on the estimation of a key parameter, the Emission Fraction F_E. The conversion method was applied on three samples containing ^{3}H, ^{14}C and ^{238}U respectively, allowing then to assess the detection efficiency of a digital radioimager, BeaQuant™. Particular attention was paid to matrix effect of contaminated material that could affect the detection efficiency. This article is coupled with a companion paper, providing support to apply the conversion method to decommissioning investigations.

Keywords

autoradiography, surface/volumetric activities, detection efficiency, Geant4, emission fraction.

Introduction

Autoradiography is a two-dimensional image of the radioactive emissions from a solid material. It appears to be one of the most suitable technique to detect, quantify and map radioactive particle emissions, with the significant advantage to be a non-destructive method [1]. The usual methods use films (silver halide emulsions or phosphor screens) which are just blackened under radiations: standard specimens are needed to quantify the blackening level. In opposition to films, the radioimagers, a new technology of Digital Autoradiography (DA), allow an acquisition in real time giving an individual particle counting (cps cm^{-2}). Developed first in biological, medical and pharmaceutical fields to track molecules labeled with radioactive tracers [1], autoradiography is now a valuable technique to study solid materials such as rock samples in geological field, building materials or personal protective equipment in a dismantling context. DA is of primary interest to study properties of rock targeted for the final disposal of spent nuclear fuel, such as the sorption and diffusion of radioactive elements into rocks [2-4]. The connected porosity of rocks which controls the diffusion process [5], can also be fruitfully investigated with DA after impregnation with the ^{14}C-PolyMethylMetAcrylate (^{14}C-PMMA), a radioactive resin. The radioactive tracer is mapped on decimeter scale samples [6-7]. In the front-end activities of the nuclear fuel cycle, DA technology is being used now to locate precisely the uranium present in a given ore, as well as the remaining radioactive elements in uranium mill tailings [8-9].

The investigation of radionuclide contaminations under dismantling processes has also been recently developed using autoradiography. A concrete floor of an old nuclear laboratory has indeed been studied with phosphor screens, to map and quantify the radioactive contaminations [10]. A full-scale visualization of the contaminations was obtained, and half of the estimated activities measured by autoradiography was consistent with the liquid scintillation counting measurements, which is a reference technique in the measurement of beta emissions [1;10-14].

For the other half of the autoradiography measurements, the observed discrepancy was due to calibration problems including two successive unit changes:

1- From DLU cm^{-2} (Digital Luminescence Unit) to Bq cm^{-2} for the analyzed surface of the contaminated sample. Contrary to digital radioimagers providing a direct particle counting per area and per time, autoradiography technique using phosphor screens gives a signal per area in the arbitrary unit DLU [10]. To convert DLU cm^{-2} into Bq cm^{-2}, standard specimens with known activities must be exposed during the same time than samples of interest.

2- From Bq g^{-1} to Bq cm^{-2} for the standard specimens. The most often, standard specimens for autoradiography consist of a set of strips whose activities are given in Bq g^{-1} (ART0123A for ^{3}H, ARC146B for ^{14}C, from ARC Inc.). So, the surface activities of these strips (Bq cm^{-2}) need to be estimated before performing the first conversion from DLU cm^{-2} to Bq cm^{-2}.

For many applications, there is also a need to estimate an activity per unit mass, when activity per unit area can be determined with autoradiography technology or with Surface Contamination Meters (SCMs), these last being widely used for decommissioning operations. Until now, this conversion remains a challenging task.

The aim of this paper is thus to provide a useful conversion technique allowing to switch simply and properly between surface and volumetric activities. This method is based on Geant4 simulations which provide the fraction of particles reaching a given surface, i.e. the Analyzed Surface of a Contaminated Volume (ASCV), among all the particles emitting in this given volume. This key parameter is known as the Emission Fraction F_E.

Three samples of rock and plastic, each contaminated with a different radionuclide (^{3}H, ^{14}C and ^{238}U series), have been used in order to illustrate the conversion from Bq cm^{-3} to Bq cm^{-2}. The emission fractions calculated with Geant4 for each sample, have allowed the conversion from the known volumetric activities to the estimated surface activities. Surface activities have also been determined experimentally using the gaseous radioimager BeaQuant™ (formerly known as Beaver™). The detection efficiency ε of this detector, which corresponds to the number of

detected particles among the number of particles emitted from the ASCV, can thus be assessed for three different radionuclides, just by comparing measured surface activities with the estimated ones.

For a given device (radioimager or SCM), the detection efficiency varies from one radionuclide to another according to the particle type and its energy of radiation. It is also possible that the instrument detection efficiency for a given radionuclide depends on the material in which it is emitted (known as "matrix effect"). More importantly, the particle counting measured with a detector depends on the contamination thickness into the material. Both effects are carefully investigated in the present work.

1. Materials and Tools

1.1. Radioimager

BeaQuant™ [15, 16], a gaseous device based on the combination of a parallel ionization multiplier with a micro pattern gas detector, was used as a digital radioimager. Samples are deposited in contact with the gas chamber, in such a manner that radioactive particles emerging from a contaminated surface of the sample (i.e. the ASCV), interact with gas (ionization), resulting in the creation of secondary electrons. Via an appropriate electric voltage applied between sample (the cathode), micromeshes and anode, secondary electrons are multiplied and then located onto the 2D pixelized anode. Then, each initial particle which triggers an electronic acquisition is reconstructed providing an autoradiography image formation in real time.

The maximal spatial resolution obtained for both ^{3}H and alpha detection is 20 μm, while the sensitivity can reach 8×10^{-4} cps cm^{-2} [15]. It can also be noted that BeaQuant™ is not affected by X or gamma rays, and that the detection response is linear with the activities and covers 5 orders of magnitude. Moreover, BeaQuant™ is able to separate alpha and beta emissions, based on a threshold applied on the energy deposited in gas (far higher for alpha than for beta), and

on the selection of adequate acquisition settings supplied by the manufacturer AI4R [15]. A sample holder called GS with a rectangular area for analysis of 12 cm by 8 cm, providing a total Detector Surface area S_D = 96 cm², was used for the measurements.

1.2. Samples

Three laboratory samples of interest were used to experimentally illustrate the proposed conversion method and determine the detection efficiency of BeaQuant™ (Figure 1).

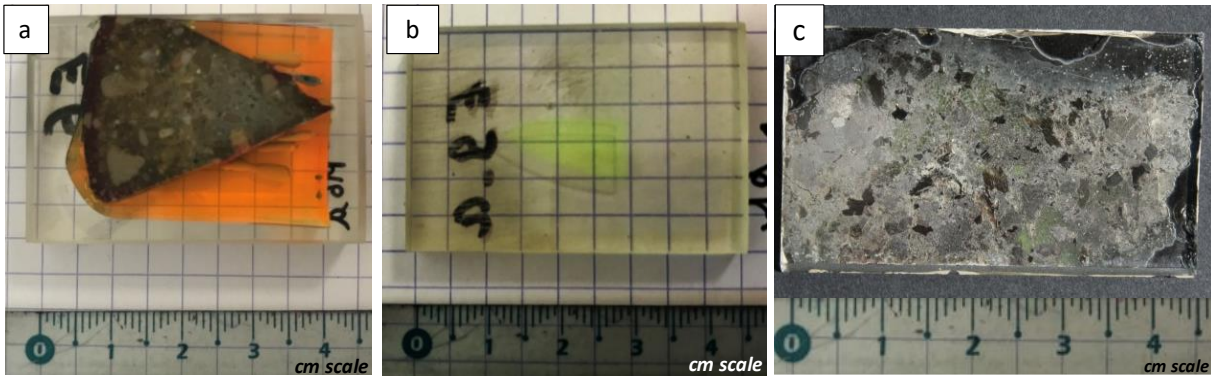

Fig. 1 Samples pictures. a- M6 sample is a triangular piece of mortar impregnated and surrounded with ^{3}H-PMMA resin (orange). b- M9 sample is a triangular piece of ^{14}C-PMMA (yellow). c- M8 sample is a thin section of granite, including *β*-uranophane (U-bearing minerals)

The first sample (M6) is a triangular piece of mortar which has been impregnated with a ^{3}H doped PMMA resin (pure beta emitter) [17]: a significant area of homogeneous pure ^{3}H-PMMA resin is also present around the mortar (orange colored zone in Figure 1a). The second sample (M9) is a sub-triangular piece (yellow zone in Figure 1b) of homogeneous resin of ^{14}C doped PMMA (pure beta emitter), surrounded by non-radioactive colorless resin. Volumetric activity of the PMMA resin is known for each of the two samples (Table 1).

Finally, the third sample (M8) is a granite thin section (rock thickness of 30 µm) sticked on a glass slide (Figure 1c). It contains natural uranium bearing minerals known as β-uranophane (54.4 wt% U) distributed in small clusters. The age of the rock (150 Ma) and alpha spectrometry attest the secular equilibrium of ^{238}U series [9]. For each ^{238}U disintegration, the 13 daughters disintegrate too, leading to the simultaneous emission of eight alpha and six beta particles, plus all the associated emissions: gamma and X-rays, Auger and conversion electrons. However, when analyzing with BeaQuant™, the option allowing counting only alpha particles has been chosen. Therefore, all the other emissions produced by ^{238}U decay chain are not investigated in this work (anyway, BeaQuant™ is not sensitive to gamma and X-rays).

A theoretical Eq. (1) proposed in [18], was employed to estimate the activity of each alpha emission from 1 cm^3 of β-uranophane crystal (i.e. the Volumetric Activity of one alpha $A_{V,\alpha 1}$): a value of 26409 Bq cm^{-3} is found (Table 1) for each alpha emission, giving a total activity for the eight alphas of 221271 Bq cm^{-3}.

$$A_{V,\alpha 1} = \rho\, \lambda \left(\frac{C_x}{100}\, \frac{\mathcal{N}}{A_x}\right) \quad (1)$$

Where ρ is the density of β-uranophane (3.9 g cm^{-3}), λ is the disintegration constant of ^{238}U (0.492×10^{-17} s^{-1}), C_X is the weight fraction of uranium in β-uranophane (54.4 wt%) measured by microprobe with a wavelength-dispersive spectroscopy system (Cameca SX100, Camparis facilities, University Pierre and Marie Curie, Paris), N the Avogradro number (mol^{-1}) and A_X the molar mass of uranium (238.029 g mol^{-1}).

Detailed features and properties of these three samples are provided in Table 1.

Table 1 Sample properties. For M8 sample, data are separated between granite rock under exponent (1) and β-uranophane under exponent (2), granite being the whole sample, β-uranophane a component of the sample

Sample	M6	M9	M8
Material	PMMA resin	PMMA resin	(1)granite (rock) (2)β-Uranophane mineral
Radionuclide	^{3}H	^{14}C	^{238}U series(2)
Chemical formula	$(C_5H_8O_2)_n$	$(C_5H_8O_2)_n$	$Ca(UO_2)_2(SiO_3OH)_2 \cdot 5H_2O$ (2)
Density ρ (g cm^{-3})	1.19	1.19	3.9 (2)
Contamination thickness d_C (µm)	7000	500	30 (1) and (2)
Approximative surface area (cm^2)	5	1	10 (1) , < 1 (2)
Known Volumetric Activity $A_{V,K}$ (Bq cm^{-3})	7 000 000	330 000	26 409 (2) *

Footnote to table 1 : * the volumetric activity given for M8 sample refers to each alpha emission of the ^{238}U decay chain. This value needs to be multiplied by the number of alpha (eight in ^{238}U series) to obtain the total activity of alphas in β-uranophane

1.3. Geant4 simulations and validation

Geant4 (GEometry ANd Tracking 4) is a powerful and C++ based toolkit allowing to simulate the transport of all kinds of particles through the matter [19]. It was used in this work to model the transport of beta and alpha particles emitted from the three samples studied here. An accurate list of the sample materials including chemical compositions (loaded in Geant4) is given in supplementary data (Table 1). Energy spectra of beta emissions have been extracted from database provided in the Rad Toolbox software developed by the Oak Ridge National Laboratory [20]. The energy distributions for the alpha emissions, have been extracted from standard [21]. Simulations have been achieved considering 10^7 beta or alpha particles, ensuring a valuable statistical analysis.

Geant4.10.02.p02 version was used for this study with a physics list based on the electromagnetic standard processes and models (EM standard physics list). The creation of a specific physics list allows to customize some settings instead of using the proposed default values.

In order to validate the implemented physics in Geant4, the Maximum Range values R_{MAX} of beta particles travelling in plastic (i.e. PMMA), concrete and steel (materials defined in supplementary data Table 1) with kinetic energy ranging from 20 keV to 1 MeV, were calculated using both ESTAR program from NIST database [22] (National Institute of Standards and Technology), and Geant4 simulations. Both tools provide similar R_{MAX} values, with linear correlations displaying a slope a close to 1 as well as a correlation coefficient R^2 of 0.99 (Figure 2a and supplementary data Table 2), except for beta radiations in steel where a = 0.7. This discrepancy might be due to additional physics processes involved in the Geant4 physics list for which the cross-sections are enhanced by high density material such as steel. The same comparison has been performed for alpha particles travelling in air, plastic and iron, using ASTAR program from NIST database [22] and Geant4: the obtained R_{MAX} values are very close as illustrated by the slope a =1 and the $R^2 > 0.98$ for the linear correlations (Figure 2b and supplementary data Table 3).

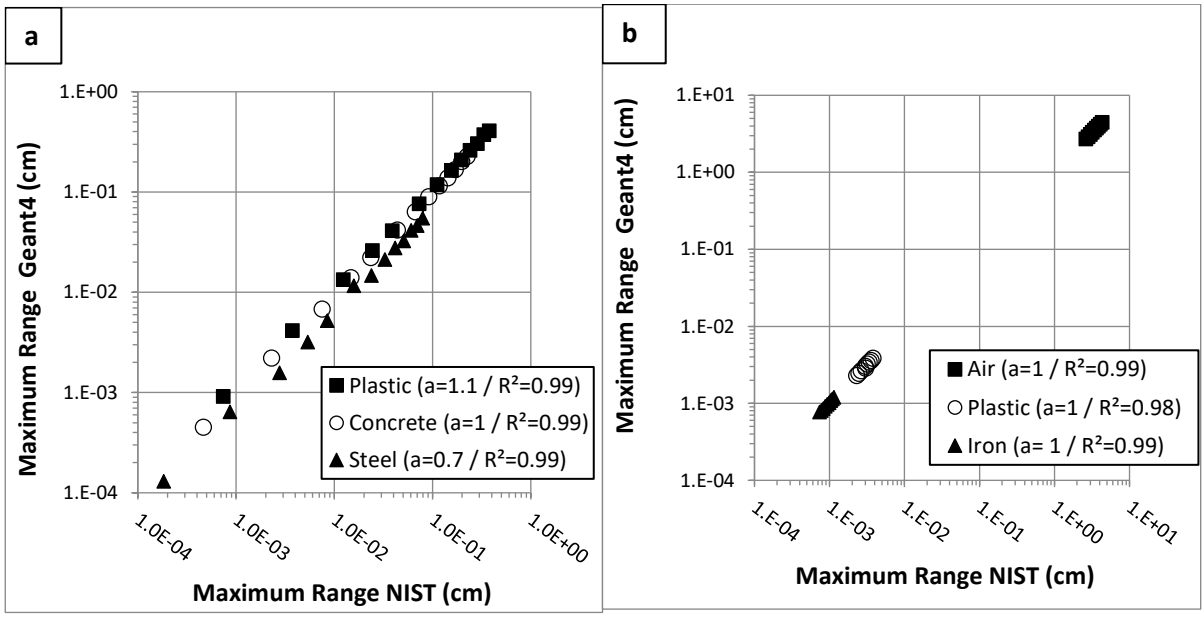

Fig. 2 Comparison of maximum range values (linear correlation with a slope "*a*" and a correlation coefficient "R^2"): NIST [22] Versus Geant4. a- beta emissions from 20 to 1000 keV. b- alpha emissions from 4000 to 5600 keV

2. Method

2.1. Detection efficiency calculation

Each radiation detector has a detection efficiency ε depending on the radiation energy and on the radiation type (alpha, beta, gamma). The geometry of the detector has also a great influence on the detection efficiency, because the solid angle of particles emissions depends on 1- the distance between the Analyzed Surface of the Contaminated Volume (ASCV) and the sensitive part of the detector, and 2- the ratio between contamination and detector surface areas. The nature of the contaminated material, i.e. the material in which particles travel, could also impact the detection efficiency. Indeed, the energy of particles, which decreases at each interaction with matter, can be different at the analyzed surface of a contaminated material A, compared to the analyzed surface of a contaminated material B, because of the matrix effect.

To determine precisely the efficiency of a SCM, the ISO standard 7503-3 [23] recommends to use calibrated sources with 10×10 cm² active area and certified alpha, beta or gamma Emission Rate *ER* in 2π (provided in counts per second (cps) for the total contaminated Surface area of the Source S_S), and to apply the following Eq. (2):

$$\varepsilon = \frac{(SCR_S - SCR_B)}{SER_S} \quad (2)$$

$$with\ SER_S = \frac{ER_S}{S_S},\ SCR_B = \frac{CR_B}{S_D},\ SCR_S = \frac{CR_S}{S_D} \quad if\ S_S > S_D, or\ SCR_S = \frac{CR_S}{S_S} \quad if\ S_D > S_S$$

where SCR_S is the Surface Count Rate measured on the calibrated Source in cps cm^{-2}, SCR_B the Surface Count Rate measured for the Background in cps cm^{-2}, SER_S the certified Surface Emission Rate in 2π of the calibrated Source in cps cm^{-2}. A Surface Count Rate *SER* being a

Count Rate CR divided by the related surface area of counting: - S_D the Surface area of the sensitive part of the Detector (cm²) or - S_S the Surface area of a calibrated Source in cm². Then, the Surface Count Rate measurement (SCR_C) of a homogeneously Contaminated surface, for which the radionuclide is known, can be corrected by the factor $1/\varepsilon$ of the corresponding radiation type and energy region to obtain the Surface Emission Rate SER_C of the Contamination (Eq. (3)).

$$SER_C = \frac{(SCR_C - SCR_B)}{\varepsilon} \quad (3)$$

$$with\ SER_C = \frac{ER_C}{S_C},\ SCR_B = \frac{CR_B}{S_D},\ SCR_C = \frac{CR_C}{S_D} \quad if\ S_C > S_D, or\ SCR_C = \frac{CR_C}{S_C} \quad if\ S_D > S_C$$

The autoradiography technology allows to map a contaminated surface to calculate its surface area value S_C: it is thus possible to choose the relevant area to calculate SCR_C from the Count Rate of the contamination CR_C (cps) (Eq. (3)). For other radioactivity detectors, generally one of the two assumptions (S_D or S_C) has to be chosen.

The detection efficiency ε of the radioimager BeaQuant™ is investigated in this work for pure beta emitters (^{3}H and ^{14}C) and for alpha emitters from the entire decay chain of ^{238}U (eight alphas). To this purpose, the three samples (see Figure 1) were used: although they are not referenced sources with certified surface emission rate in 2π, volumetric activities of M6 and M9 samples were determined in laboratory by liquid scintillation counting (Table 1). For the M8 sample, the theoretical Eq. (1) proposed by [18] was used to estimate the volumetric activity of each alpha emitter of uranium bearing minerals, as already stated above. Surface activities have been estimated from these volumetric activities, in order to be compared with BeaQuant™ surface measurements.

2.2. Concept of Emission Fraction F_E

The ISO standard 7503-1 [24] proposes to use an Emission Fraction F_E to convert Surface Emission Rate *SER* (cps cm^{-2}) into Surface Activity A_S (Bq cm^{-2}) (Eq. (4)).

$$A_S = \frac{SER_C}{F_E} = \frac{(SCR_C - SCR_B)}{\varepsilon F_E} \quad (4)$$

F_E is the ratio between the number of particles emerging from the ASCV (or in other terms the face of a contaminated sample in contact with the detector window) and the number of particles produced in the contaminated volume. However, the concept of F_E presented in [24] is based on the assumption that the contamination layer is infinitely thin, eliminating the concept of volume. Accordingly, the 2π geometry yields to a reduction of the detectable emissions by a factor of 2 [23], providing an estimation of F_E equal to 0.5. However, in the case of thick contaminations, which is the general case found for nuclear wastes or geological samples, such an assumption induces a significant bias between Surface Activity A_S and Volumetric Activity A_V. In other terms, Eq. (4) proposed in the ISO standard 7503-1 [24] to calculate A_S, is not truly adapted to thick contaminated samples when considering F_E = 0.5.

Emission Probability P_E, described as the ratio between the number of particles created and the number of decays of the same radionuclide, is equal to 1 for the three samples analyzed with BeaQuant™. Indeed, M6 and M9 are pure beta emitters (^{3}H and ^{14}C). Concerning M8 in which only alpha particles are considered, P_E could be considered equal to 1 for each of the eight alpha emissions of the ^{238}U decay chain. In this work, P_E equal to 1 (i.e. cps = Bq) allows the direct conversion from the measured Surface Count Rate SCR_C (cps cm^{-2}) to the Surface Activity A_S (Bq cm^{-2}), after correction from the corresponding instrument efficiency ε and from the background measurement, without having to involve the Fraction Emission F_E (Eq. (5)).

$$A_S = \frac{SCR_C - SCR_B}{\varepsilon} = SER_C \quad (5)$$

In the present study, an appropriate estimation of F_E is used to calculate a Volumetric Activity A_V in Bq cm^{-3} (next section 2.3.), instead of a Surface Activity A_S in Bq cm^{-2} of a contamination layer infinitely thin (as proposed in [24] and Eq. (4)).

The Emission Fraction F_E is difficult to estimate because it depends on the nature of the contaminated material (matrix), the radionuclide (particle type and emission energy) and the Contamination thickness d_C. The contamination is considered as homogeneous in the whole material. For a given d_C, the denser the material is, the lower the number of particles of a given type and energy emerge on the ASCV. For a same material, high energy beta particles are able to cross over longer distances than low energy betas or alphas. This leads to a higher value of F_E considering the same Contaminated thickness d_C. Finally, for a given combination of a material and a radionuclide, the greater d_C is, the lower will be the fraction F_E of particles emerging from the total volume, through the ASCV. Indeed, particles are more likely to be stopped in a thick material, before to reach the ASCV, than in a thin one. A proper simulation procedure using Geant4 has been performed to answer to these difficulties.

2.3. Estimation of the Emission Fraction F_E using Geant4 simulations

A contaminated material can be depicted as a parallelepiped object (Figure 3a), in which three thicknesses are defined: 1- apparent Object thickness d_O (which can be considered as infinite in the case of contaminated floor and/or wall), 2- Contamination thickness d_C (Figure 3a), corresponding to the depth of the contamination, 3- Maximum Range R_{MAX} of the particles responsible of the contamination in the considered material.

Knowing that d_O is thus necessarily greater or equal to dc, d_O is not a significant thickness in the present work, while d_C needs to be known. R_{MAX} can be lower, equal or higher than d_C. If $R_{MAX} < d_C$, a part of the contaminated volume is not explored by the autoradiography technique

(or by any other SCM), because particles emitted deeper than the maximum range cannot reach the ASCV (Figure 3b). Thus, it is not relevant to estimate F_E for contamination thicknesses $d_C > R_{MAX,}$ even if it could happen in real samples.

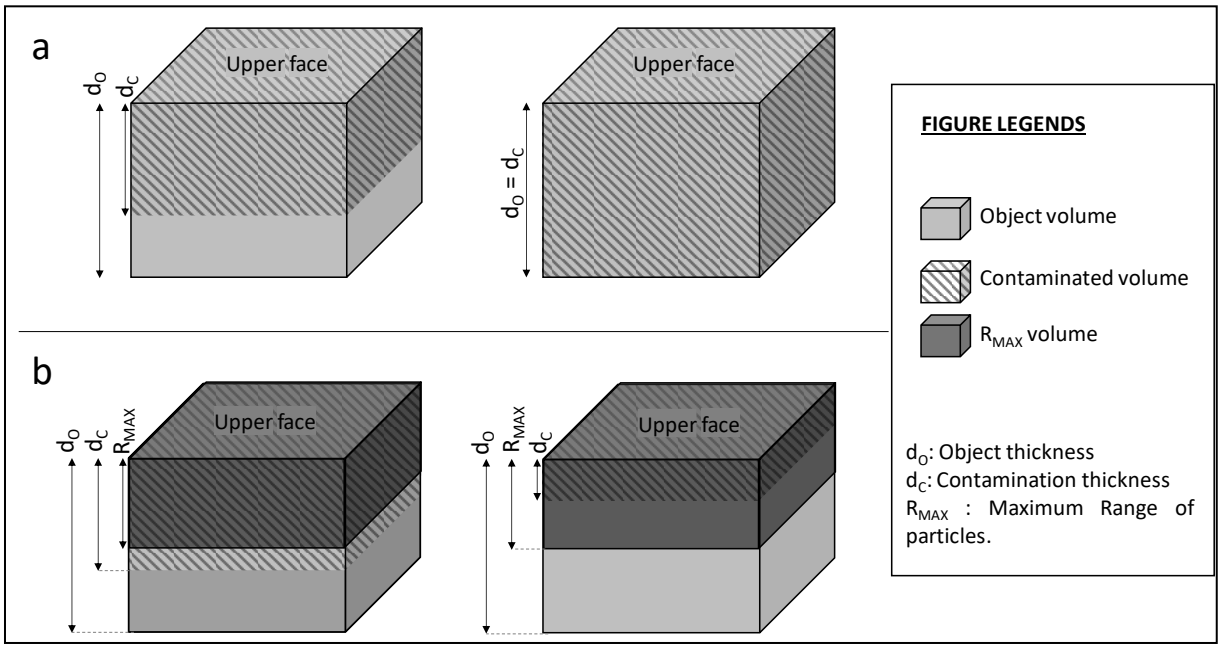

Fig. 3 Definitions of important thicknesses for a contaminated sample. The upper face corresponds to the Analyzed Surface of the Contaminated Volume (ASCV). a- The Contamination thickness d_C is lower or equal to the Object thickness d_O. b- The Maximum Range R_{MAX} can be lower, equal or greater than the Contamination thickness d_C

Geant4 was used to calculate the fraction F_E of the volumetric activity detectable on the ASCV, for the three studied samples previously described in section 1.2. F_E will then allow to switch from volumetric to surface activities.

The first step consisted to calculate with Geant4, the R_{MAX} values in the given material, using the maximal emission energy of the considered radiation [20, 21]. Then, a rectangular parallelepiped of $4 \times R_{MAX}$ in width, $4 \times R_{MAX}$ in length and $2 \times R_{MAX}$ in height, filled with the

material to consider, was build (Figure 4). Into this volume, 10^7 particles corresponding to one of the studied radionuclides have been generated with initial random directions and positions in a segment. This segment ranges from the origin (0, 0, 0) to the point (0, 0, $-R_{MAX}$) (see Figure 4). These conditions and dimensions were chosen in order that any emitted particle can possibly reach the upper face of the material volume, i.e. the ASCV. For each emitted particle, the initial kinetic energy is selected in the corresponding energy distribution [20, 21]. The fraction of particles emerging at the ASCV, according to their emission depth h, was calculated, h ranging from the surface (h = 0) to $h = -R_{MAX}$. Then, an integral calculation has been achieved to estimate the fraction of particles reaching the ASCV, i.e. the emission fraction according to the thickness d of the considered layer, $F_E(d)$. The numerical Steps s of $F_E(d)$ are adjusted according to the order of magnitudes of the R_{MAX} values: s = 0.01 µm for ^{3}H, s = 0.1 µm for ^{14}C and the alpha emitters of the ^{238}U decay chain.

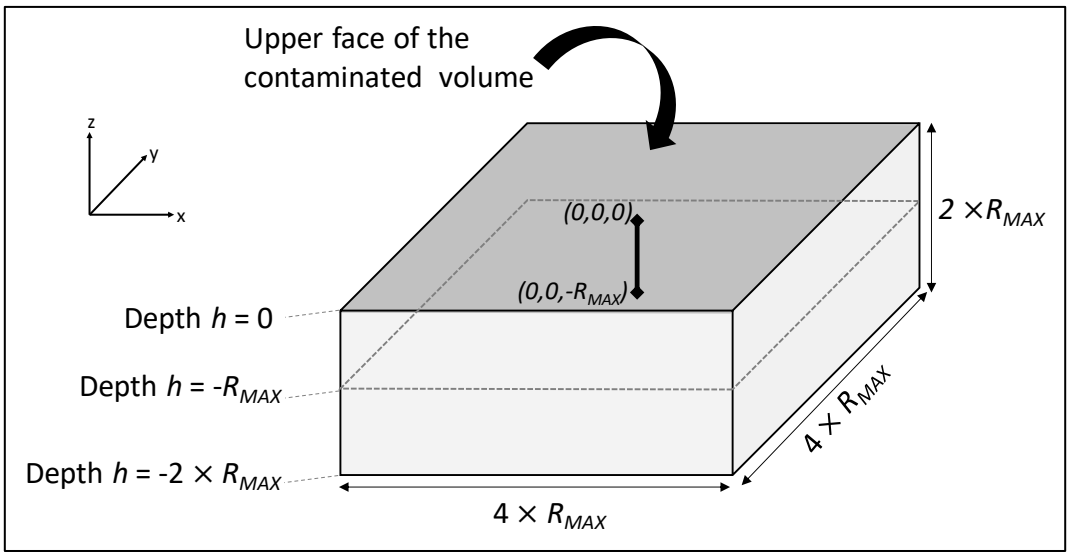

Fig. 4 Scheme of the geometry chosen in the Geant4 simulations. The parallelepiped object corresponds to the contaminated volume centered in (0, 0, $-R_{MAX}$). The upper face, i.e. the Analyzed Surface of the Contaminated Volume (ASCV), is centered in (0, 0, 0). Particles are emitted from the segment ranging from (0, 0, 0) to (0, 0, $-R_{MAX}$)

With these sets of F_E values, it is then possible to evaluate the Surface Activity A_S (in Bq cm^{-2}) of a sample with known Volumetric Activity A_V (in Bq cm^{-3}), and conversely. For a given case (a material and a radiation type), if the Contamination thickness $d_C > R_{MAX}$, the activities need to be calculated with a thickness equal to R_{MAX}, and $F_E(R_{MAX})$ has to be used (Eq. (6a)). Otherwise, if $d_C < R_{MAX}$, activities have to be calculated with $F_E(d_C)$ (Eq. (6b)).

$$A_{S,G} = A_{V,K} \times F_E(R_{MAX}) \times R_{MAX} \quad or \quad A_{V,G} = \frac{A_{S,K}}{F_E(R_{MAX}) \times R_{MAX}} \quad if\ d_C > R_{MAX} \qquad (6a)$$

$$A_{S,G} = A_{V,K} \times F_E(d_c) \times d_c \quad or \quad A_{V,G} = \frac{A_{S,K}}{F_E(d_c) \times d_c} \quad if\ d_C < R_{MAX} \qquad (6b)$$

Where $A_{S,G}$ is the Surface Activity estimated with Geant4 simulation tool (Bq cm^{-2}), $A_{V,K}$ the Known Volumetric Activity (Bq cm^{-3}), $A_{V,G}$ the Volumetric Activity estimated with Geant4 simulation tool (Bq cm^{-3}) and $A_{S,K}$ the Known Surface Activity (Bq cm^{-2}). Obviously, the important assumption of the model is to consider that the activity is homogeneously distributed in the volume.

Surface activities of calibrated sources are generally known to calculate the detection efficiency of a detector (Eq. (2)), but for controlled samples (the case in the present work), surface activities needed to be evaluated from their known volumetric activities (Eq. (6)): application of the conversion from Bq cm^{-3} to Bq cm^{-2}. Then for any contaminated material with P_E =1, the measured Surface Count Rate SCR_C can be converted into volumetric activity (Eq. (6)), after detection efficiency correction (Eq. (5)): use of the conversion from Bq cm^{-2} to Bq cm^{-3}. However, this last assumption is accurate only if the detection efficiency of the instrument is independent of any matrix effect.

2.4. Method for evaluating the matrix effects on detection efficiency

In this section, the impact of the contaminated material type on the detection efficiency of a given instrument is examined. Indeed, it is not trivial to know if the detection efficiency of a radionuclide obtained on a calibrated source or a well characterized sample (Eq. (2)) can be employed to determine the surface activity of a contaminated object emitting the same radionuclide (Eq. (5)), but composed with another material.

To clarify this point, it is necessary to determine the kinetic energy distribution of the emitted particles when they reach the ASCV. Indeed, for almost all the common radiation detectors, and in this work for autoradiography devices, the detection efficiency is directly linked to the energy of the particles.

Geant4 was used to plot the frequency distribution (fd) of the kinetic energy of particles (beta and alpha) just as they go out from the ASCV, considering three different materials: plastic, concrete and steel. In these simulations, the contaminated material is still depicted as a rectangular parallelepiped $4 \times R_{MAX}$ long and width, and a thickness (height) of $2 \times R_{MAX}$ (R_{MAX} of the considered radionuclide in one of the chosen materials (Figure 4)). A second series of simulations has also been achieved with contaminated volume presenting a constant Contamination thickness d_C, regardless of the material.

Finally, it is important to emphasize that the matrix effect described here is only related to the detection efficiency of a given instrument, i.e. the ratio of the number of particles detected to the number of particles emitted at the ASCV. The number of particles emitted at the ASCV, given by the Emission Fraction F_E, is however strongly dependent on the nature of the material, as previously explained (end of the section 2.2.)

3. Results and discussion

3.1. Surface Count Rate measurements with BeaQuant™

Each of the three samples M6, M8 and M9 was acquired with the radioimager BeaQuant™ during one hour, in beta mode for M6 and M9, and in alpha mode for M8. On the autoradiographs obtained, the Contaminated Surface areas S_C on which the count rate measurements were performed are outlined with a white frame (Figure 5). S_C values (cm²) are given in Table 2, together with the count rates measured. To calculate the Surface Count Rate (SCR_C), note that S_C are always lower than S_D (Detector Surface area) in the present work.

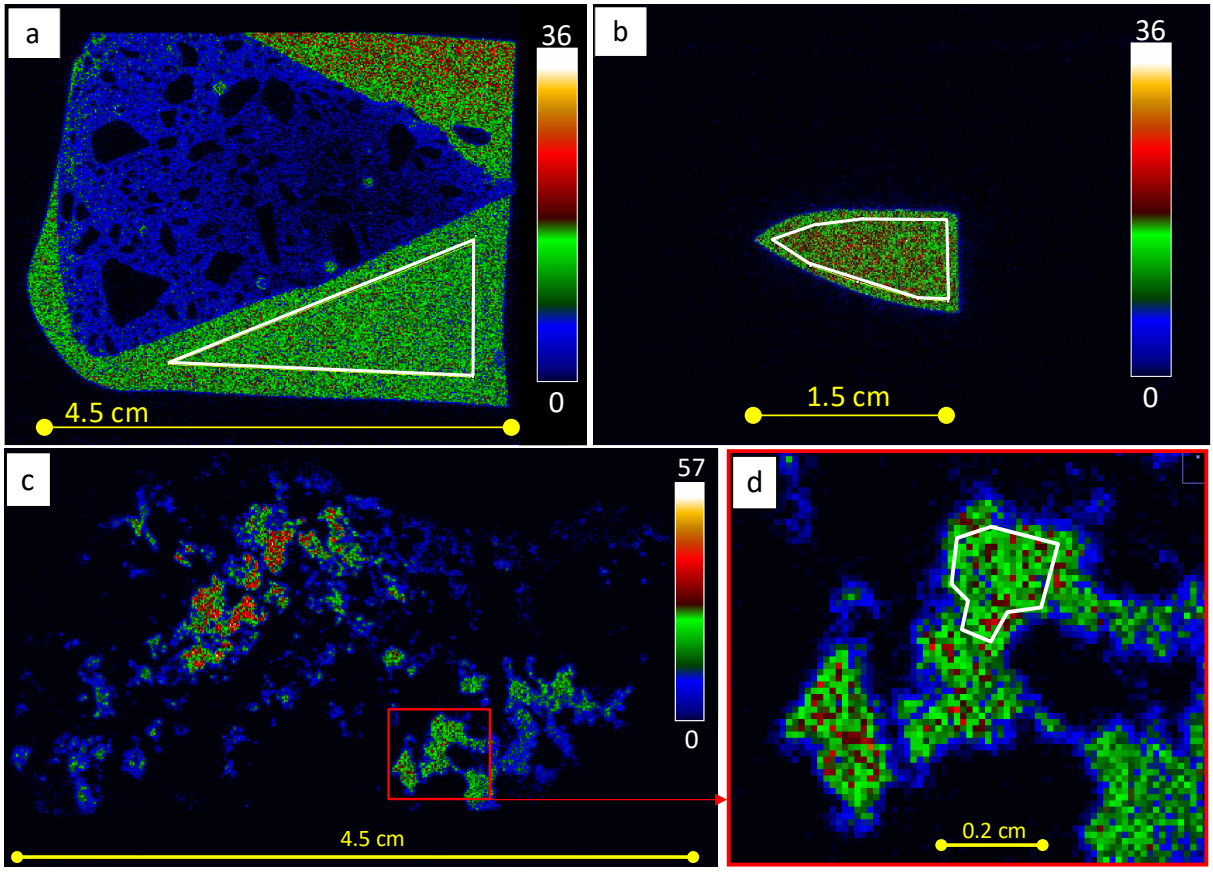

Fig. 5. a- Autoradiography of the beta emissions from the M6 sample, a mortar (triangular shape in blue and black) impregnated with ^{3}H-PMMA resin. Resin surrounds also the mortar (in green and red). b- Autoradiography of the beta emissions from a triangular piece of ^{14}C-PMMA (M9 sample). c- Autoradiography of the alpha emissions from uranium bearing minerals (β-uranophane) included in the granite M8. D- Zoom on the red frame of image c.

Autoradiographs are acquired with BeaQuant™ and with the GS 12 × 8 cm² sample holder. Color scales give the particle counts in 1 hour, pixel size is fixed at 100 µm and surface count rate measurements have been performed on the surface areas delimited with a white frame

In M6 sample, the mortar corresponds to the central triangular area which is heterogeneous (Figure 5a). It is a mixture of non-radioactive grains (in black) and pores filled with the radioactive resin ^{3}H-PMMA (in blue). The two homogenous areas surrounding the mortar are made of pure ^{3}H-PMMA resin, on which the measurement was performed. The M9 sample shows a sub-triangular and homogeneous piece of ^{14}C-PMMA resin (Figure 5b). Then, the autoradiography of M8 sample depicts the spatial distribution of the β-uranophane crystals into the rock (Figure 5c); a nearly homogeneous and small area corresponding to a cluster of β-uranophane crystals was chosen to perform the measurement (Figure 5d).

Table 2 Measurements of the three samples with BeaQuant™ using the GS 12 × 8 cm² sample holder: Contamination Surface area S_C, Count Rate of this surface CR_C and Surface Count Rate SCR_C

Sample	Radionuclide	Particle	Used setting	S_C (cm²)	CR_C (cps) for S_C	SCR_C (cps cm^{-2})
M6	^{3}H	beta	beta	$1.00 \times 10^{+00}$	38.21	38.10
M9	^{14}C	beta	beta	6.29×10^{-01}	30.09	47.85
M8	^{238}U decay chain	alpha	alpha	2.51×10^{-02}	1.60	63.90

Blank measurements were also performed in order to obtain the Background Surface Count Rate of the detector (SCR_B), using the sample holder GS (12 × 8 cm^2) and the two different acquisition settings (Table 3). These blank values, needed to the further calculations of the

detection efficiency of BeaQuant™ (Eq. (2)), are typically 4 to 5 orders of magnitude lower than the three samples surface count rates.

Table 3 Background measurements of BeaQuant™ (GS 12 × 8 cm² sample holder). Detector Surface area S_D, Background Count Rate CR_B and Background Surface Count Rate SCR_B

Setting	S_D (cm²)	CR_B (cps) for S_D = 96 cm²	SCR_B (cps cm^{-2})
beta	96	2.65	2.76×10^{-02}
alpha	96	0.13	1.35×10^{-03}

3.2. Surface Emission Rate estimations: from Bq cm^{-3} to Bq cm^{-2}

The Volumetric Activities ($A_{V,K}$) in Bq cm^{-3} are known for the M6 and M9 samples, and calculated for each alpha emission of the M8 sample (due to the secular equilibrium of the ^{238}U decay chain, all the daughters have the same activity) (Tables 1 and 4). The conversion method has been applied to estimate the Surface Activity ($A_{S,G}$) in Bq cm^{-2} of the three samples, i.e. convert the Bq cm^{-3} (Table 1) into Bq cm^{-2}, using Eq. (6). Because P_E of ^{14}C, ^{3}H and each alpha of the ^{238}U decay chain are equal to 1, these estimated Surface Activities $A_{S,G}$ are equal to the Surface Emission Rate SER_C (i.e. Bq = cps). The comparison between the Surface Count Rates (SCR_C) measured previously with BeaQuant™ and these estimated Surface Emission Rates (SER_C) would allow then to assess the detection efficiency of BeaQuant™ (next section), using Eq. (2). The three samples are indeed used as calibrated sources.

As previously mentioned, the first step of the conversion method is the calculation of the maximum ranges of particles emitting in the three samples. These R_{MAX} values are displayed in Table 4, with the related maximum energy used.

Table 4 Estimation of the Surface Activity $A_{S,G}$ of the M6, M8 and M9 samples (since $P_E = 1$, $A_{S,G} = SER_C$ (Surface Emission Rate in cps cm^{-2})). The Known Volumetric Activities $A_{V,K}$ and the Contamination thicknesses d_C have been reported from Table 1. Maximum Ranges values R_{MAX} have been calculated with Geant4, using the maximum energy also reported. According Eq. (6), the Emission Fraction F_E is calculated for the smaller of the two, between d_C and R_{MAX}: for M6 and M9 samples, $F_E(R_{MAX})$ is used to perform the conversion Bq cm^{-3} to Bq cm^{-2}, while for M8 sample $F_E(d_C)$ is used

Sample	**Material**	**Radionuclide**	**Particle**	**Known Volumetric Activity $A_{V,K}$ (Bq cm^{-3})**	**Contamination thickness d_C (cm)**	**Maximum Energy (keV)**	**Maximum Range R_{MAX} (cm)**	**Emission Fraction $F_E(d_C)$**	**Emission Fraction $F_E(R_{MAX})$**	**Estimated Surface Activity $A_{S,G}$ (Bq cm^{-2})** (or SER_C (cps cm^{-2}))
M6	PMMA	^{3}H	beta	7 000 000	7×10^{-01}	18.6	8.40×10^{-04}	-	0.026	153
M9	PMMA	^{14}C	beta	330 000	5×10^{-02}	156.5	2.78×10^{-02}	-	0.034	312
M8 – ^{238}U Decay Chain	β–Uranophane mineral	^{238}U	alpha	26 409	3×10^{-03}	4198	1.73×10^{-03}	0.138	-	11
		^{234}U	alpha	26 409	3×10^{-03}	4775	2.09×10^{-03}	0.166	-	13
		^{230}Th	alpha	26 409	3×10^{-03}	4687	2.03×10^{-03}	0.162	-	13
		^{226}Ra	alpha	26 409	3×10^{-03}	4784	2.10×10^{-03}	0.167	-	13
		^{222}Rn	alpha	26 409	3×10^{-03}	5490	2.57×10^{-03}	0.204	-	16
		^{218}Po	alpha	26 409	3×10^{-03}	6002	2.92×10^{-03}	0.233	-	19
		^{214}Po	alpha	26 409	3×10^{-03}	7687	4.23×10^{-03}	0.316	-	25
		^{210}Po	alpha	26 409	3×10^{-03}	5304	2.44×10^{-03}	0.192	-	15
		Average alpha					**$2{,}51 \times 10^{-03}$**	**0.197**		

	∑ alpha	**211 272**	**125**

406

407

408

Then the Emission Fraction F_E has been calculated with Geant4. As the Contamination thicknesses d_C of the M6 and M9 samples (0.7 cm and 0.05 cm respectively) are higher than the maximum range of the corresponding radiation in PMMA (8.4×10^{-4} cm for M6 and 2.78×10^{-2} cm for M9), F_E was estimated in a volume of thickness R_{MAX} (Table 4). Concerning the M8 sample, as the Maximum Ranges R_{MAX} of the eight alphas (Table 4) are of the same order of magnitude than the sample Contamination thickness d_C (3×10^{-3} cm), the Emission Fraction F_E of each alpha has been estimated for the Contamination thickness d_C (Table 4). Thus, the Surface Activities $A_{S,G}$ (= SER_C since $P_E = 1$) presented in Table 4 are calculated with Eq. (6a) for M6 and M9 samples, and with Eq. (6b) for each alpha of M8 sample. The sum of the alphas activity has been performed in order to be compared with the total alphas counting measured with BeaQuant™.

To conclude, it is crucial to always consider that autoradiographic method remains a surface measurement technique. For the analyzed samples of the present work, the Contamination depths d_C were higher or equal to R_{MAX}. In the case of samples with $d_C < R_{MAX}$, $F_E(d)$ for ^{3}H and ^{14}C radionuclides emitted in PMMA (plastic), concrete and steel are provided from $d = 0$ to $d = R_{MAX}$ in the companion paper [25]. However, the analysis of a sample where d_C is unknown can be problematic, especially if $d_C < R_{MAX}$. The unique way to solve properly that issue would be to determine d_C by measuring the contamination profile as a function of depth.

3.3. Detection efficiency calculation of BeaQuant™

Comparing surface count rate measurements with surface emission rate estimations (Eq. (2)), the detection efficiency of BeaQuant™ (sample holder reference GS), can be calculated for the three samples which substitute the calibrated sources in the present work (Table 5). In the M6 sample emitting ^{3}H in PMMA (plastic), 25% of the particles emitted through the ASCV are detected, whereas only 15% of betas emitted from ^{14}C-PMMA (M9 sample) are collected.

Concerning ^{238}U decay chain, alphas emitted in the β-uranophane crystals (M8 sample) are detected with an efficiency of 51%.

Table 5 Instrument efficiencies ε of BeaQuant™ using the GS 12 × 8 cm² sample holder. After correction from the Background Surface Count Rate SCR_B, the Surface Count Rate SCR_C is compared to the Surface Emission Rate SER_C expected for the samples (Eq. (2))

Sample	Radionuclide	Particle	Used setting	SCR_C (cps cm^{-2})	SCR_B (cps cm^{-2})	SER_C (cps cm^{-2})	ε
M6	^{3}H	beta	beta	38.10	2.76×10^{-02}	153	0.25
M9	^{14}C	beta	beta	47.85	2.76×10^{-02}	312	0.15
M8	^{238}U decay chain	alpha	alpha	63.90	1.35×10^{-03}	125	0.51

3.4. Matrix effect for the detection efficiency calculation

Figure 6 represents the frequency distributions (fd) of the kinetic energy for particles emitted from the upper face of a contaminated volume (i.e. the ASCV), in different matrix types. For alpha and beta, these fd are quite similar for a given radionuclide emission passing through the three different materials, regardless of the contamination thickness. Indeed, simulations were achieved considering two cases. In the first case, the thickness of the contaminated volume was set to $R_{MAX,}$ which is variable from one material to another (Figure 6 and supplementary data Figure 1). In the second case, a constant thickness higher than R_{MAX} (30 µm, 100 µm and 1 mm for ^{3}H, ^{238}U and ^{14}C respectively) was used for each radionuclide, independently of the material (supplementary data Figure 2).

For more clarity, only one example of beta and alpha emitters is displayed in Figure 6.

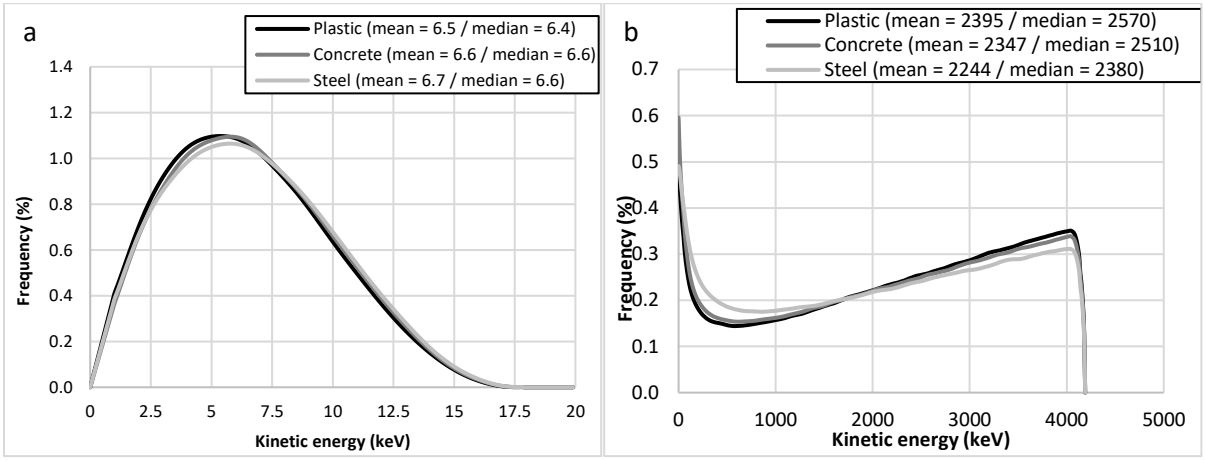

Fig. 6 Frequency distributions (fd) of the kinetic energy of particles when reaching the Analyzed Surface of the Contaminated Volume (ASCV), supplied for three different materials: plastic; concrete and steel. The mean and median values of the kinetic energy are given for each fd. a- ^{3}H radionuclide (beta emission), contamination thickness = R_{MAX}. b- ^{238}U radionuclide (alpha emissions only), contamination thickness = R_{MAX}

For beta emissions, a slight increase of mean and median energy values when material density increases (from plastic to steel) is observed, with a maximum relative standard deviation of 6 %. For alpha emissions, mean and median energy values decrease in denser materials, with a maximum relative deviation of 5 %. It can also be concluded that the detection efficiency of a given detector is the same for a given combination alpha/energy or beta/energy, regardless of the nature of the contaminated material. It means that the matrix effect on the detection efficiency of a given detector is very low or even negligible for the considered alpha and beta emissions.

4. Conclusion

Autoradiography can be an efficient technique to measure traces of radioactivity on the surface of materials for biological and geological research fields but also more increasingly in the

471 framework of decommissioning. However, the calibration step is always an important issue, as
472 with all common Surface Contamination Meters (SCM).

473 The activity of standard specimens, needed to calibrate the autoradiography signal from films,
474 are most of the time provided in Bq g^{-1}, which is not consistent with the signal measured on
475 autoradiographs (DLU cm^{-2} for phosphor screens, grey level per pixel for silver halide
476 emulsions). The conversion tools proposed in the present work improve the calibration step for
477 these traditional methods of autoradiography.

478 Concerning radioimagers and SCMs, calibrated sources with certified surface emission rate are
479 often used to evaluate the detection efficiency needed to calibrate the instrument or to correct
480 the measurements. However, this kind of source are not easy to obtain (long national
481 procedures, usage regulations, transport…). Often it is necessary to use well characterized and
482 available laboratory samples, as is the case for the present study. Geant4 allowed to estimate
483 the Emission Fraction $F_{E,}$ used to evaluate the Surface Activity A_S (or Surface Count Rate *SCR*,
484 since $P_E = 1$) of the three laboratory samples chosen here, knowing their volumetric activities:
485 this illustrated the use of the conversion from Bq cm^{-3} to Bq cm^{-2} (Eq. (6)).

486 Results have demonstrated the importance of a good estimation of the emission fraction F_E to
487 apply the conversion method. Indeed, even if a contamination layer is extremely thin, F_E is
488 somewhat different from 0.5 (i.e. 50% of particles reaching the ASCV), as considered in the
489 ISO standard 7503-1 [24]. As an example, beta particles from ^{3}H have a short range in plastic:
490 for a contamination thickness equal to the relevant R_{MAX} = 8.3 µm, around 3 % of betas can
491 reach the ASCV (i.e. $F_E(R_{MAX} = 8.3\ \mu m) = 0.03$). While the thickness of β-uranophane (the U-
492 bearing mineral including in the M8 sample) of 30 µm induces fraction emissions ranging from
493 0.14 to 0.32 according the alpha particle considered among the eight emitted in the ^{238}U decay
494 chain (i.e. $0.14 < F_E(30\ \mu m) < 0.32$) (Table 5). The companion paper [25] supplies data of F_E
495 to deal with the cases where Contamination thickness $d_C < R_{MAX.}$ $F_E(d)$ are also provided from

thickness $d = 0$ to $d = R_{MAX}$ of the considered particle type/energy and material. These $F_E(d)$ are given for three materials (plastic, concrete and steel) and for ^{3}H, ^{14}C and ^{238}U, as well as other radionuclides that can be encountered in nuclear dismantling facilities.

It was subsequently possible to calculate the detection efficiency of a radioimager, BeaQuant™ (GS 12 × 8 cm^2 sample holder), for the three laboratory samples used as calibrated source in this work. Since it has been shown than for a given instrument, the detection efficiency of both beta/energy or alpha/energy combinations is independent of the composition of the material contaminated (i.e. no matrix effect), the detection efficiency found for the three samples can be generalized to the concerned radionuclides: $\varepsilon = 25\%$ for ^{3}H, $\varepsilon = 15\%$ for ^{14}C, $\varepsilon = 51\%$ for alpha emitters in ^{238}U decay chain. These efficiency values ε can be used to calibrate or correct BeaQuant™ measurements on materials contaminated with ^{3}H, ^{14}C or ^{238}U (Eq. (3)), performed in the same configuration as used in the present study. Indeed, the detection efficiency of BeaQuant™ is strongly dependent of the holder type and of the electric fields applied in the detector (defined in the acquisition settings) (manufacturer's data). As an example, [9] found a detection efficiency greater than 80% for alpha emitters in ^{238}U decay chain, using another sample holder.

After detection efficiency correction (Eq. (3)), F_E parameter can be used to convert a measured surface activity into volumetric activity (Eq. (6)). Such conversion remains nowadays a challenge in decommissioning investigations where activity per gram is systematically required to suitably manage the nuclear wastes. That is why we propose in the companion paper, a second part "From Bq cm^{-3} to Bq cm^{-2} (and conversely) - Part 2: a useful conversion for decommissioning operations", to provide a large set of data helping to deal with the conversion problems possibly encountered in a dismantling context.

Acknowledgements

This work was performed within the Investments for the future program of the French Government and operated by the French National Radioactive Waste Management Agency (Andra). We would like to thank the reviewers for their constructive comments and criticisms in reviewing the paper, and Alain Meunier for his thorough re-reading of this article.

References

1. L'Annunziata MF (2012) Handbook of radioactivity analysis. Academic Press, Third edition

2. Ittner T, Allard B (1990) Diffusion of strontium, technetium, iodine and cesium in granitic rock. Radiochim. Acta, 49:101-106

3. Pinnioja S, Jaakkola T, Miettinen JK (1984) Comparison of batch and autoradiographic methods in sorption studies of radionuclides in rock and mineral samples. Mater Res Soc Symp Proc. 26:979–984

4. Muuri E, Sorokina T, Donnard J, Billon S, Helariutta K, Koskinen L, Martin A, Siitari-Kauppi M (submitted in 2018) Electronic autoradiography of ^{133}Ba particle emissions; diffusion profiles in granitic rocks. Appl. Radiat. Isot.

5. Voutilainen M, Siitari-Kauppi M, Sardini P, Kekäläinen P, Muuri E, Timonen J, Martin A (2017) Modelling transport of cesium in Grimsel granodiorite with heterogenous structure and dynamic update of Kd. Water Resources Research. 53:9245-9265

6. Hellmuth KH, Lukkarinen S, Siitari-Kauppi M (1994) Rock matrix studies with carbon-14-polymethylmethacrylate (PMMA); method development and applications. Isotopenpraxis Isotopes in Environmental and Health Studies. 30:47-60

543 7. Siitari-Kauppi M (2002) Development of ^{14}C-polymethylmethacrylate method for the
544 characterisation of low porosity media: Application to rocks in geological barriers of nuclear
545 waste storage. Academic Dissertation, Report Series in Radiochemistry 17

546 8. Angileri A, Sardini P, Donnard J, Duval S, Lefeuvre H, Oger T, Patrier P, Rividi N, Siitari-
547 Kauppi M, Toubon H, Descostes M (2018). Mapping ^{238}U decay chain equilibrium state in
548 thin sections of geo-materials by digital autoradiography and microprobe analysis. Appl.
549 Radiat. Isot. 140:228-237

550 9. Sardini P, Angileri A, Descostes M, Duval S, Oger T, Patrier P, Rividi N, Siitari-Kauppi M,
551 Toubon H, Donnard J (2016) Quantitative autoradiography of alpha particle emission in geo-
552 materials using the Beaver™ system. Nucl. Instrum. Methods Phys. Res. A, 833:15-22

553 10. Leskinen A, Fichet P, Siitari-Kauppi M, Goutelard F (2013) Digital autoradiography (DA)
554 in quantification of trace level beta emitters on concrete. J. Radioanal. Nucl. Chem. 298:153-
555 161

556 11. Fichet P, Bresson F, Leskinen A, Goutelard F, Ikonen J, Siitari-Kaupi M (2012) Tritium
557 analysis in building dismantling process using digital autoradiography. J. Radioanal. Nucl.
558 Chem. 291:869-875

559 12. Haudebourg R, Fichet P (2016) A non-destructive and on-site digital autoradiography-based
560 tool to identify contaminating radionuclide in nuclear wastes and facilities to be dismantled.
561 J. Radioanal. Nucl. Chem. 309:551–561

562 13. ISO 7503-2 (2016) Measurement of radioactivity –Measurement and evaluation of surface
563 contamination - Part 2: Test method using wipe tests

564 14. ISO 9698 (2010) Water quality – Determination of tritium activity concentration – liquid
565 scintillation counting method

15. BeaQuant™ - Real-time autoradiography http://www.ai4r.com/ Accessed 22 Sep 2018

16. Donnard J, Berny R, Carduner H, Leray P, Morteau E, Provence M, Servagent N, Thers D (2009) The micro-pattern gas detector PIM : A multi-modality solution for novel investigations in functional imaging. Nucl. Instrum. Methods Phys. Res. A, 610 :158-160

17. De La Asuncion (2005) Caractérisation de la porosité des matériaux cimentaires avec la methode 14C-polyméthylmétacrylate (14C-PMMA). French master thesis of the university of Poitiers and of the institute national des sciences appliqués de Toulouse, 81pp

18. Ilic R, Durrani SA (2003) Solid State nuclear track detector (Chapter 3). In : L'Annunziata MF (ed) Handbook of Radioactivity Analysis, 2nd edn, Elsevier Science, USA, pp. 179-237, pp. 1273

19. Agostinelli S, Allison J, Amako KA, Apostolakis J, Araujo H, Arce P, Asai M, Axen D, Banerjee S, Barrand G, Behner F, Bellagamba L, Boudreau J, Broglia L, Brunengo A, Burkhardt H, Chauvie S, Chuma J,... & Zschiesche D (2003) GEANT4 - a simulation toolkit. Nucl. Instrum. Methods Phys. Res. A, 506:250-303

20. Eckerman KF, Sjoreen AL (2004) Radiological toolbox user's manual. United States. Department of Energy

21. Laboratoire National Henri Becquerel, Library for gamma and alpha emissions http://www.lnhb.fr/nuclear-data/module-lara/. Accessed 6 May 2018

22. Berger MJ, Coursey JS, Zucker MA (1999) ESTAR, PSTAR, and ASTAR: Computer programs for calculating stopping-power and range tables for electrons, protons, and helium ions (version 1.21). https://www.nist.gov/pml/stopping-power-range-tables-electrons-protons-and-helium-ions. Accessed 14 Jul 2018

23. ISO 7503-3 (2016) Measurement of radioactivity. Measurement and evaluation of surface contamination- Part 3: Apparatus calibration

590 24. ISO 7503-1 (2016) Measurement of radioactivity- Measurement and evaluation of surface
591 contamination- Part 1: General principles

592 25. Billon S, Sardini P, Leblond S, Fichet P, (in press 2019) From Bq cm^{-3} to Bq cm^{-2} (and
593 conversely)- part 2: a useful conversion for decommissioning operations. Journal of
594 Radioanalytical and Nuclear Chemistry